

# Improved Analysis of Gridline TLM Pattern Including Effect of Uncontacted Gridlines

Daniel L. Meier , Member, IEEE, Vinodh Chandrasekaran, Member, IEEE, and Brian J. Meier 

**Abstract**—Contact resistivity ( $\rho_c$ ) for silicon solar cells is often measured using a pseudo-TLM pattern of equally spaced gridlines, which is cut from the cell itself. In this measurement, the uncontacted (floating) gridlines between two contacted gridlines are usually assumed to be disconnected from the silicon sheet. Analysis of such TLM data yields an approximate value of  $\rho_c$ , which is reasonably accurate for  $L_T/L > 1$ , but increasingly less accurate for  $L_T/L < 1$  (good contacts). In this article, the TLM analysis is extended to explicitly include the effect of uncontacted gridlines to provide a more accurate analysis of gridline TLM data. Three contact systems were measured and then analyzed by both the approximate and improved methods. In all cases, a commercial Ag paste was screen printed and fired through a dielectric coating ( $\text{SiN}_x/\text{AlO}_x$  or  $\text{SiN}_x$ ) to contact a  $\text{p}^+$ -poly (p-TOPCon) layer, an  $\text{n}^+$ -poly (n-TOPCon) layer, or a  $\text{p}^+$ -boron (p-diffused) layer. The improved TLM analysis gave  $\rho_c$  values of 3.51, 0.89, and 5.26  $\text{m}\Omega\cdot\text{cm}^2$ , respectively. Analysis of the n-TOPCon data is complicated by 2-D current flow across the tunneling oxide and into the n-substrate, with corresponding uncertainty. Expressions for converting  $\rho_c$  to a component of series resistance are also given. Additional calculations were carried out to determine  $\rho_c$  error with approximate TLM analysis. With assumed  $L_T/L$  values of 1, 0.5, and 0.25, the errors are 3.7%, 41%, and 280%, respectively.

**Index Terms**—Contact resistivity, gridline, TLM measurement, series resistance, silicon, solar cell.

## I. INTRODUCTION

CONTACT resistance, associated with the interface between a semiconductor substrate and its metal contact, is an important parameter in many electronic devices. This is particularly true for metal gridlines on silicon solar cells, since some of the cell's power must be sacrificed to force current through this resistance. Shockley [1] is credited with first recognizing that current traveling laterally passes from a semiconductor sheet into a contact over a characteristic distance, called the current transfer length ( $L_T$ ), and for devising a method for measuring contact resistivity ( $\rho_c$ ) using this distance and the semiconductor

sheet resistance ( $R_{\text{sh}}$ ) as

$$\rho_c = R_{\text{sh}} L_T^2. \quad (1)$$

According to Shockley's formulation, valid for a contact with length ( $L$ ) much greater than the current transfer length ( $L/L_T \gg 1$ ), the contact resistance ( $R_c$ ) is equivalent to the resistance of an additional length ( $L_T$ ) of semiconductor sheet

$$R_c = R_{\text{sh}} (L_T/Z) \quad (2)$$

where  $Z$  is the dimension along the contact and perpendicular to the contact length.

By modeling the contact as a lossy transmission line, Berger [2] was able to extend the expression for contact resistance to cases where the contact length ( $L$ ) may not be greater than the transfer length ( $L_T$ ) as

$$R_c = R_{\text{sh}} (L_T/Z) \coth(L/L_T). \quad (3)$$

Note that for  $L \gg L_T$  (wide contact),  $R_c = \rho_c/(L_T Z)$ , whereas for  $L \ll L_T$  (narrow contact),  $R_c = \rho_c/(LZ)$ .

Berger also proposed a test structure and analysis method for determining both  $R_{\text{sh}}$  and  $R_c$ . His test structure is the genesis of what today is called the TLM pattern for measuring contact resistivity. TLM can be understood to mean either "transmission line model" (per Berger) or "transfer length method" (per Shockley). Although the  $\coth(L/L_T)$  term appears frequently in the literature for narrow contacts, it is difficult to find a derivation. For completeness, a derivation is provided in the appendix. Schroder and Meier gave a comprehensive overview of ohmic contacts on solar cells, including physical mechanisms at work and contact resistivity data [3].

TLM is the standard technique for measuring the contact resistivity of solar cell contacts. The conventional TLM pattern comprises a set of parallel metal bars, usually wide (large  $L$ ) bars to facilitate probing and analysis ( $L/L_T \gg 1$ ), having different spacings between adjacent bars [4]. This means that conventional TLM patterns must be defined on "witness" wafers that are processed along with the solar cell wafers. In addition to the need for these extra witness wafers, questions arise as to the validity of applying measurements done on witness wafers to the analysis of actual solar cells. Differences between the conventional TLM pattern and the solar cell gridline pattern, particularly in line (bar) width and thickness as well as line spacing, may cause the two patterns to respond differently to contact paste rapid firing, for example. In that case, contact resistivity obtained from TLM witness wafers may not truly represent contact resistivity of the actual solar cell contacts.

Manuscript received May 18, 2020; revised July 9, 2020 and August 28, 2020; accepted September 2, 2020. Date of publication September 23, 2020; date of current version October 21, 2020. (Corresponding author: Daniel L. Meier.)

Daniel L. Meier and Brian J. Meier are with Lightdrop Harvest, LLC, St. Marys, PA 15857 USA (e-mail: dmeier@lightdropharvest.com; bmeier@lightdropharvest.com).

Vinodh Chandrasekaran was with the Heraeus Precious Metals North America, Photovoltaic Global Business Unit, West Conshohocken, PA 19428 USA. He is now with the First Solar, Perrysburg, OH 43551 USA (e-mail: vinodh.chandrasekaran@firstsolar.com).

Color versions of one or more of the figures in this article are available online at <https://ieeexplore.ieee.org>.

Digital Object Identifier 10.1109/JPHOTOV.2020.3022697



Fig. 1. Photograph of a gridline TLM pattern, as cut from a solar cell. Sample width is 10 mm and length is 35 mm.

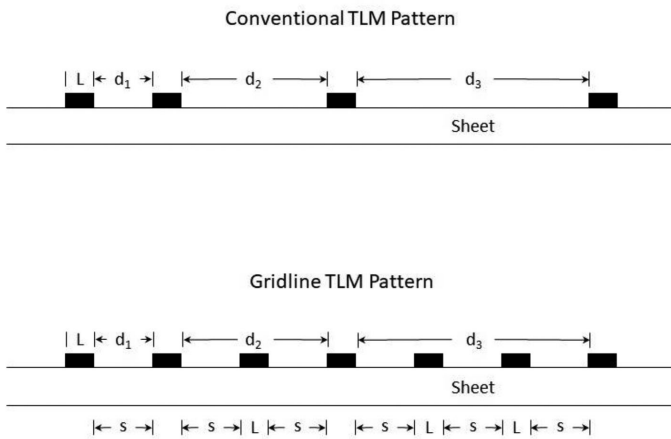


Fig. 2. Difference between conventional TLM pattern and gridline TLM pattern.  $Z$  is the dimension of the bar (gridline) into the paper.  $R_{sh}$  is the semiconductor sheet resistance.

Because of these difficulties and concerns, the conventional TLM pattern has largely been supplanted by the gridline TLM pattern for measuring solar cell contact resistivity [5]. This pattern is so-named because the test sample, usually about 10 mm wide, is cut from a finished solar cell with the gridlines forming the bars in a ladderlike pattern. A typical test sample, shown in Fig. 1, has a number of parallel gridlines. Measurements made on such a test sample are truly representative of the gridlines in the cell, since the bars (gridlines) of the test sample have undergone actual cell processing conditions and perfectly represent the dimensions, spacing, and interface properties of cell gridlines.

Fig. 2 shows how a gridline TLM pattern can mimic a conventional TLM pattern. Bar-to-bar resistance associated with the  $n$ th set of bars in a conventional TLM pattern is

$$R_n = R_{sh} [(d_n/Z) + (2L_T/Z) \coth(L/L_T)] \quad (4)$$

where  $d_n$  is the spacing between bars in the  $n$ th pair. A gridline TLM pattern is similar with

$$d_n = ns + (n - 1)L \quad (5)$$

where  $s$  is the (constant) edge-to-edge spacing between adjacent bars (gridlines). Another way to express  $d_n$  is  $d_n = np - L$ , where  $p$  is the pitch (center-to-center distance) of the gridlines.

A plot of  $R_n$  versus  $d_n$  is used in the conventional TLM pattern to determine  $R_{sh}$  from the slope and  $2R_c$  from the y-intercept of a fitted straight line. A similar plot can be made for the gridline TLM pattern. However, in this case, the impact of the

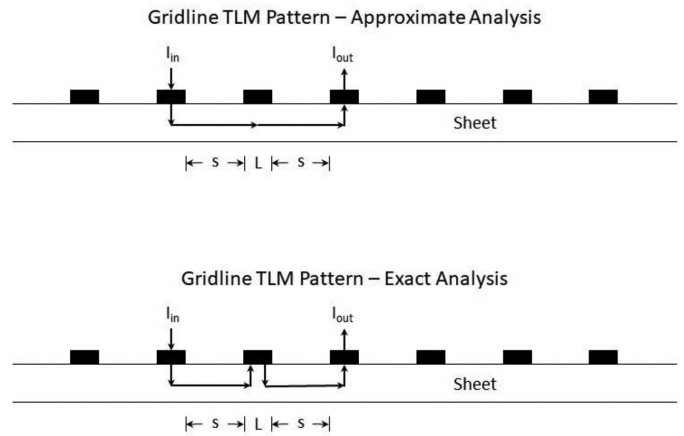


Fig. 3. Illustration of current flow in a gridline TLM pattern for an approximate analysis (uncontacted gridline electrically disconnected from semiconductor sheet) and for an exact analysis (uncontacted gridline communicates with sheet).

uncontacted (floating) bars is not properly taken into account, as the entire current is assumed to stay within the semiconductor sheet as shown in the upper portion of Fig. 3. In reality, some of the current will pass from the sheet into the bar and then back into the sheet, as shown in the lower portion of Fig. 3.

In a TLM measurement of resistance, current is forced across the bar/sheet interface of the input bar ( $I_{in}$ ) and is extracted from the output bar ( $I_{out}$ ) after being forced across that bar/sheet interface. In an approximate analysis of the TLM resistance data, the uncontacted gridline (bar) is simply treated as a length  $L$  of sheet material with resistance  $R_{bar} = R_{sh}(L/Z)$ . This approach ignores any current that may transfer from the sheet into the uncontacted bar and back out into the sheet again. In an exact analysis of the TLM resistance data, this current transfer is recognized, and the uncontacted bar (and directly underlying sheet) is treated as a resistance element, with  $R_{bar} < R_{sh}(L/Z)$ . The exact analysis always gives a lower contact resistivity than the approximate analysis, but the difference is small if  $L_T > L$  (3.7% at  $L_T = L$ , reducing to 0.05% at  $L_T = 3L$ ). However, if  $L_T < L$ , the difference can become quite large (41% at  $L_T = \frac{1}{2}L$ , increasing to 280% at  $L_T = \frac{1}{4}L$ ). This means that for a good contact ( $L_T < L$ ), an exact analysis must be done to obtain an accurate value of contact resistivity. For modest to poor contacts ( $L_T > L$ ), an approximate analysis is sufficient. In all cases, the contact metal is assumed to have zero resistance (i.e., negligible compared to  $R_{sh}$ ).

Other researchers have recognized that uncontacted (unprobed) gridlines introduce errors into the gridline TLM analysis. In one case [6], with screen-printed Ag contacts, no current is assumed to flow in the uncontacted gridlines, so  $R_{bar} = R_{sh}(L/Z)$ . In another case [7], with Ni/Cu-plated contacts, current is assumed to transfer entirely and abruptly into and out of the uncontacted gridlines, so  $R_{bar} = 0$ . An exact expression for  $R_{bar}$ , which falls between these two extremes, is developed in the next section.

It should be noted that the term ‘‘exact,’’ as referenced above, applies only to the treatment of current flow in uncontacted

gridlines. The analysis presented in this article is idealized in that the resistance of the contact bars is assumed to be zero, the semiconductor sheet is taken to be thin (small compared to the contact length ( $L$ )), and the sheet resistance is assumed to be uniform (same beneath the contact as beside it). These assumptions are valid in many cases, but not all. For example, if the semiconductor sheet is in contact with a substrate of the same type (e.g.,  $n^+n$ ) with no p-n junction isolation, current also flows in the substrate and a more sophisticated (2-D) analysis is needed. Similarly, if another source of resistance besides the contact resistance (e.g., a tunneling oxide) is present in the current path, a more sophisticated analysis is again required to avoid including that extraneous resistance with the metal/silicon contact resistance. Some variability in sheet resistance and contact resistivity throughout the test pattern is inevitable, and will be reflected in scatter in the data and associated errors in the fitted parameters.

## II. THEORY

Expanding the analysis of gridline TLM resistance data to include not only the two contacted bars but also any uncontacted bars between them requires an expression for the resistance associated with an uncontacted bar. Such an expression, which properly accounts for the division of current between the silicon sheet and the uncontacted bar, can be found in [8] as

$$R_{\text{bar}} = \Delta V_{\text{bar}}/I_0 = (2L_T/Z) R_{\text{sh}} \tanh[L/(2L_T)]. \quad (6)$$

Equation (6) follows directly from [8, eq. (9)] after simplifications associated with the sheet resistance of the metal bar (typically  $\approx 0.001 \Omega/\square$ ) being insignificant compared to the sheet resistance of the silicon sheet layer (typically  $\approx 100 \Omega/\square$ ) and differences in nomenclature ( $a \rightarrow L_T$  and  $2W \rightarrow L$ ) are applied.  $R_{\text{bar}}$  can be evaluated in two limits. For poor contacts ( $L_T/L \gg 1$ ),  $\tanh[L/(2L_T)] \approx L/(2L_T)$  and so  $R_{\text{bar}} \approx R_{\text{sh}} (L/Z)$ . For good contacts ( $L_T/L \ll 1$ ),  $\tanh[L/(2L_T)] \approx 1$  and  $R_{\text{bar}} \approx R_{\text{sh}} (2L_T/Z)$ , which approaches 0 for very good contacts. Thus,  $R_{\text{bar}}$  ranges from 0 (current transfers entirely to bar) to  $R_{\text{sh}} (L/Z)$  (current remains entirely in sheet), as required.

Equation (6) has also been derived from a TLM for a silicide contact to a silicon diffused layer for integrated circuit applications [9, eq. (35)]. A test pattern, consisting of a series of unprobed bars, was then used to measure  $\rho_c$  for  $\text{TiSi}_2$  contacting a silicon-implanted/diffused layer [10] and for  $\text{NiSi}$  and  $\text{PtSi}$  contacting a silicon-implanted/diffused layer [11]. These two independent derivations [8], [9] put (6), which is central to the exact analysis of the gridline TLM pattern, on a firm footing.

The TLM for the uncontacted bar (gridline) on a thin silicon sheet is given in Fig. 4. Note that the gridline is assumed to have zero resistance. Expressions for current traveling in the gridline as a function of position ( $I_1(x)$ ) and for current traveling in the sheet as a function of position ( $I_2(x)$ ) are taken from [8, Fig. 3].

Plots of current in the bar and current in the sheet as a function of position are given in Fig. 5(a) and (b). Note that  $I_1(x)/I_0 + I_2(x)/I_0 = 100\%$ , since total current must be divided between the bar and the sheet at any position. These plots show that current

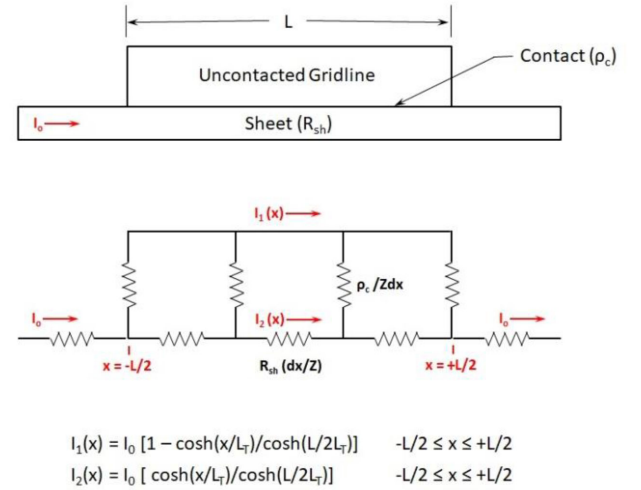


Fig. 4. TLM of an uncontacted bar (gridline) with equations for current as a function of position.

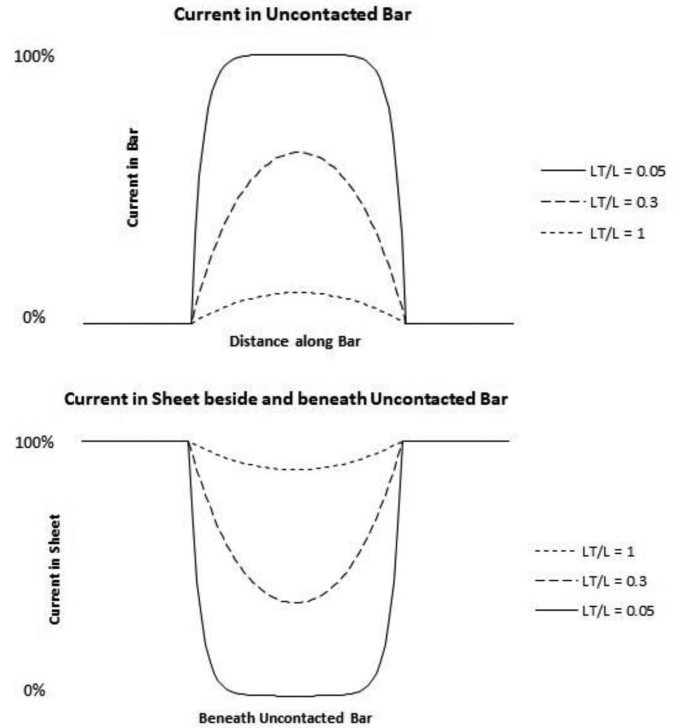


Fig. 5. (a) Fraction ( $I_1(x)/I_0$ ) of current traveling in an uncontacted bar as a function of position beneath bar for three values of relative current transfer length ( $L_T/L$ ). Current rises from zero at left edge of bar ( $x = -L/2$ ) and falls back to zero at right edge of bar ( $x = +L/2$ ). (b) Fraction ( $I_2(x)/I_0$ ) of current traveling in sheet as a function of position for three  $L_T/L$  values.

transfers mainly to the bar for a very good contact ( $L_T/L = 0.05$ ), but stays largely in the sheet for a modest contact ( $L_T/L = 1$ ).

Exact expressions for resistance values can now be written for the gridline TLM pattern of Fig. 2. The resistance between two contacted bars in the  $n$ th set is

$$R_n = R_{\text{sh}} (ns/Z) + (n-1) R_{\text{bar}} + (2L_T/Z) R_{\text{sh}} \coth(L/L_T) \quad (7)$$

where  $s$  is the (fixed) inner edge-to-edge spacing between two adjacent bars as shown in Fig. 2. Substituting for  $R_{\text{bar}}$  from (6) and rearranging yields

$$R_n(n) = \{R_{\text{sh}}(s/Z) + 2R_{\text{sh}}(L_T/Z) \tanh[L/(2L_T)]\}n + \{2R_{\text{sh}}(L_T/Z)(\coth[L/L_T] - \tanh[L/(2L_T)])\}. \quad (8)$$

As can be seen from (8),  $R_n$  is a linear function of  $n$  with

$$\text{slope} = R_{\text{sh}}(s/Z) + 2R_{\text{sh}}(L_T/Z) \tanh[L/(2L_T)] \quad (9)$$

$$\text{intercept} = 2R_{\text{sh}}(L_T/Z) (\coth[L/L_T] - \tanh[L/(2L_T)]). \quad (10)$$

A set of  $(n, R_n)$  data points can now be plotted as  $R_n$  versus  $n$  and fitted to a straight line to determine slope ( $\Omega/\text{bar}$ ) and y-intercept ( $\Omega$ ). Here,  $n$  represents the number of bars the second contacted bar is removed from the first contacted bar (or the number of fixed spaces ( $s$ ) between contacted bars). The two parameters to be extracted from this fit are  $R_{\text{sh}}$  and  $L_T$  so that  $\rho_c$  can be calculated from (1). ( $Z$ ,  $s$ , and  $L$  are known constants from the gridline TLM test sample.) Equations (9) and (10) are transcendental equations in the unknowns  $R_{\text{sh}}$  and  $L_T$ . This coupled pair of equations must be solved numerically for the two unknowns.

Following the methodology in [8], the contribution of contact resistivity to the series resistance of the cell (normalized to unit area) can be expressed as follows:

$$r_{\text{series}}(\text{contact}) = \rho_c / [L / (2b)] = \rho_c / f \quad (\text{if } L_T \geq L/2) \quad (11)$$

$$r_{\text{series}}(\text{contact}) = \rho_c / [L_T / b] \quad (\text{if } L_T \leq L/2) \quad (12)$$

where  $2b$  is the gridline pitch ( $p$ ) and  $f$  is the fraction of cell area covered by gridline metal. Note that at  $L_T = L/2$  (crossover point), both equations give the same value for  $r_{\text{series}}(\text{contact})$ . Equation (11) is familiar for the case of poor contacts. Equation (12) is applicable for good contacts. Two different equations are required because current enters a gridline in a solar cell in two different ways, depending on  $L_T/L$ . If  $L_T/L$  is large, currents collected from both sides of the gridline combine below the gridline and enter the gridline uniformly across the full contact area. If  $L_T/L$  is small, current collected to the left of the gridline enters the gridline along its left edge and current collected to the right of the gridline enters the gridline along its right edge, so the full contact area is not utilized. These expressions are useful in calculating the loss of fill factor and efficiency due to contact resistivity.

### III. DATA AND COMPARATIVE ANALYSIS

Contact resistivity was measured for three candidate contact systems, all involving screen-printed and fired Ag contacts. A gridline TLM pattern was used, and the set of resistance measurements underwent both an approximate analysis and an exact analysis. Contact structures are summarized in Table I along with the commercial Ag pastes from Heraeus that were used. A typical Ag contact pattern with gridlines and busbars was printed, with 1.6-mm gridline pitch. Starting wafers were n-Cz,

TABLE I  
STRUCTURES CONTACTED BY SCREEN-PRINTED Ag

Sample	Ag Paste	Structure
p-diffused	SOL 9370A	Ag/SiN <sub>x</sub> /AlO <sub>x</sub> /p <sup>+</sup> diffused/ n-substrate
n-TOPCon	SOL 7200N	Ag/SiN <sub>x</sub> /n <sup>+</sup> poly/tunnel oxide/ n-substrate
p-TOPCon	SOL 7100P	Ag/SiN <sub>x</sub> /AlO <sub>x</sub> /p <sup>+</sup> poly/tunnel oxide/ n-substrate

1–3  $\Omega\cdot\text{cm}$ , 180  $\mu\text{m}$  thick, 156 mm pseudosquare. Ag pastes were fired through an SiN<sub>x</sub>/AlO<sub>x</sub> stack to contact a boron-diffused emitter (SOL 9370A) in sample “p-diffused” or to contact a p<sup>+</sup> poly layer (SOL 7100P) in sample “p-TOPCon.” Another Ag paste was fired through an SiN<sub>x</sub> dielectric to contact an n<sup>+</sup> poly layer (SOL 7200N) in sample “n-TOPCon.” Note that the p-diffused and the n-TOPCon (tunnel oxide passivated contact) samples together make a p<sup>+</sup>nn<sup>+</sup> solar cell with a passivating rear contact. Such a cell structure generated considerable interest upon its introduction because of its 23.0% reported efficiency [12]. More recent work with the same structure has increased the efficiency to 25.7% with  $V_{\text{oc}}$  of 725 mV [13]. The p-TOPCon sample represents a passivating rear contact on an n<sup>+</sup>pp<sup>+</sup> cell.

In all cases, a gridline TLM sample was removed from the processed wafer by scribing part way through the wafer from the back side with a dicing saw, then breaking at the scribe line to cleave cleanly through the p<sup>+</sup>n or the n<sup>+</sup>n junction. Preparing the sample in this way precludes the formation of shunts, which complicate TLM data analysis [5], as Ag from the gridlines is not smeared along the edge of the sample and junctions are not damaged. Samples are nominally 10 mm wide and 156 mm long, a section of which is shown in Fig. 1.

Contact resistance test data were acquired using a commercial tool from GP Solar called the 4-TEST (four-point probe measurement of resistance) [14]. Similar commercial tools for TLM measurements are also available from other equipment vendors [15], [16]. The GP Solar tool uses six adjacent bars (gridlines) on a gridline TLM sample to obtain a total of 30 resistance data points. There are 5 combinations where the second bar in the measurement is 1 bar removed from the first bar, 4 combinations where the second bar is 2 bars removed from the first bar, 3 combinations with 3 bars removed, 2 combinations with four bars removed, and 1 combination with 5 bars removed for a total of 15 combinations. Allowing current to flow in both directions from bar to bar doubles the number of data points to 30. The measured resistances ( $R_n$ ) are presented in Table II for sample p-TOPCon. This gridline TLM sample had a width ( $Z$ ) of 7.304 mm, gridline pitch ( $p$ ) of 1.6 mm, and gridline length ( $L$ ) of 68.28  $\mu\text{m}$  to give an edge-to-edge spacing between gridlines ( $s = p - L$ ) of 1.531 mm, with measuring current ( $I_0$ ) of 10 mA. This value of  $I_0$  approximates solar cell current with the cell biased at its maximum power point. In Table II, the bar number ( $n$ ) is used in the exact analysis and the distance ( $d_n$ ) is used in the approximate analysis.

A plot of  $R_n$  versus  $n$  is given in Fig. 6 for the 30 data points of Table II along with its fitted line. With the fitted slope

TABLE II  
GRIDLINE TLM DATA ACQUIRED FOR SAMPLE P-TOPCON

Bar Number (n)	Distance $d_n$ (mm)	Measurement Pair	$R_n$ ( $\Omega$ )
1	1.531	1-2	49.42
1	1.531	2-1	49.45
1	1.531	2-3	48.60
1	1.531	3-2	48.64
1	1.531	3-4	48.32
1	1.531	4-3	48.35
1	1.531	4-5	49.14
1	1.531	5-4	49.17
1	1.531	5-6	46.84
1	1.531	6-5	46.87
2	3.131	1-3	97.49
2	3.131	3-1	97.55
2	3.131	2-4	96.40
2	3.131	4-2	96.45
2	3.131	3-5	96.63
2	3.131	5-3	96.69
2	3.131	4-6	95.09
2	3.131	6-4	95.14
3	3.131	1-4	145.17
3	4.731	4-1	145.26
3	4.731	2-5	144.60
3	4.731	5-2	144.69
3	4.731	3-6	142.47
3	4.731	6-3	142.56
4	6.331	1-5	193.24
4	6.331	5-1	193.40
4	6.331	2-6	190.31
4	6.331	6-2	190.46
5	7.931	1-6	238.81
5	7.931	6-1	239.00

(47.70  $\Omega$ /bar) and intercept (0.9012  $\Omega$ ),  $R_{sh}$  and  $L_T$  can be determined by solving (9) and (10) numerically. Because  $L_T \ll s$  and  $0 \leq \tanh[L/(2L_T)] \leq 1$ , (9) can be approximated as slope  $\approx R_{sh}$  ( $s/Z$ ) so that an initial guess for  $R_{sh}$  can be given as

$$R_{sh} \approx \text{slope} (Z/s) \quad (13)$$

or  $R_{sh} \approx (47.70 \text{ } \Omega/\text{bar})(0.7304 \text{ cm}/\square)/(0.1531 \text{ cm}/\text{bar})$ , so  $R_{sh} \approx 227.5 \text{ } \Omega/\square$ . This value of  $R_{sh}$  is then substituted into (10) for the fitted intercept to give

$$0.9012 \text{ } \Omega = 2R_{sh} (L_T/Z) (\coth[L/L_T] - \tanh[L/(2L_T)]). \quad (14)$$

With  $R_{sh}$  of 227.5  $\Omega/\square$ , (14) is solved numerically for  $L_T$  to give a value of 39.49  $\mu\text{m}$  to complete the first iteration. This value of  $L_T$  is substituted into (9) to solve for a refined value of  $R_{sh}$ , which is then substituted into (10) to obtain a refined value of  $L_T$ . This completes the second iteration. After three iterations, the values for  $R_{sh}$  and  $L_T$  converge, as shown in Table III. The contact resistivity can then be calculated from (1) as 3.510  $\text{m}\Omega \cdot \text{cm}^2$ . This is considered to be an exact value of contact resistivity since uncontacted bars were included explicitly in the analysis.

### Resistance Data from 4-TEST Tool

Gridline TLM Sample: p-TOPCon

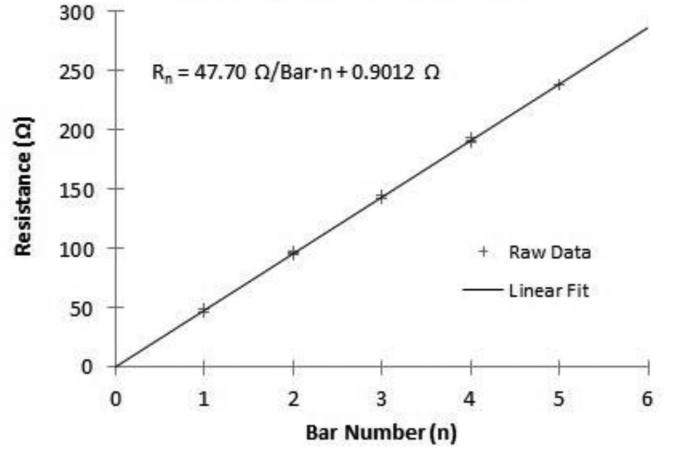


Fig. 6. Plot of 30 ( $n, R_n$ ) data points from Table II for gridline TLM sample p-TOPCon with linear fit.

TABLE III  
SUMMARY OF ITERATION RESULTS FOR SAMPLE P-TOPCON

Iteration	$R_{sh}$ ( $\Omega/\square$ )	$L_T$ ( $\mu\text{m}$ )
1	227.5	39.49
2	219.6	39.98
3	219.5	39.99

Standard numerical techniques can also be used to solve (9) and (10) together. In this case, initial guesses for both  $R_{sh}$  and  $L_T$  are needed. The initial guess for  $R_{sh}$  can be obtained from the slope using (13), as above, to give 227.5  $\Omega/\square$ . The initial guess for  $L_T$  can be obtained from the intercept as follows:

$$R_{sh}L_T^2 = \rho_c \approx (\text{intercept}/2) LZ \quad (15)$$

$$L_T \approx \sqrt{(\text{intercept}/2) (LZ/R_{sh})} \quad (16)$$

to give  $L_T \approx 31.43 \mu\text{m}$  as a starting guess. A numerical solver is then able to arrive directly at the same final result as given in Table III, but without successive iterations.

If the uncontacted bars are ignored in the analysis, an approximate value of  $\rho_c$  is obtained from the same set of resistance data. In this case,  $R_n$  is plotted against  $d_n$  (see Table II) and fitted to a straight line as expressed in (4)

$$R_n(d_n) = (R_{sh}/Z) d_n + (2R_{sh}L_T/Z) \coth(L/L_T). \quad (17)$$

$R_{sh}$  is obtained directly from the fitted slope

$$\text{slope} = R_{sh}/Z. \quad (18)$$

$L_T$  can then be determined from the fitted intercept by solving the transcendental equation

$$\text{intercept} = (2R_{sh}L_T/Z) \coth(L/L_T). \quad (19)$$

This was done and the results for the approximate TLM analysis are given in Table IV, along with results of the improved analysis. (Note that a plot of  $R_n$  versus  $d_n$  with fit is automatically generated by the 4-TEST tool, along with results of the

TABLE IV  
COMPARISON OF APPROXIMATE TLM ANALYSIS WITH IMPROVED ANALYSIS  
FOR SAMPLE P-TOPCON ( $L = 68.3 \mu\text{m}$ )

Parameter	Approximate TLM Analysis	Improved TLM Analysis
$R_{sh} (\Omega/\square)$	218	$219 \pm 0.3\%$
$L_T (\mu\text{m})$	44.8	$40.0 \pm 23\%$
$\rho_c (\text{m}\Omega\text{-cm}^2)$	4.37	$3.51 \pm 46\%$
$L_T/L$	0.656	0.586

TABLE V  
COMPARISON OF APPROXIMATE TLM ANALYSIS WITH IMPROVED ANALYSIS  
FOR SAMPLE N-TOPCON ( $L = 98.6 \mu\text{m}$ )

Parameter	Approximate TLM Analysis	Improved TLM Analysis
$R_{sh} (\Omega/\square)$	43.4	$43.9 \pm 0.6\%$
$L_T (\mu\text{m})$	67.4	$61.3 \pm 25\%$
$\rho_c (\text{m}\Omega\text{-cm}^2)$	1.98	$0.89 \pm 50\%^*$
$L_T/L$	0.684	0.621

\* The cited value of  $0.89 \text{ m}\Omega\text{-cm}^2$  is an estimate after attempting to correct for 2D current flow in the  $n^+$ /oxide/ $n$  structure; the simpler (and inaccurate) 1D analysis yields a value of  $1.65 \text{ m}\Omega\text{-cm}^2$ .

TABLE VI  
COMPARISON OF APPROXIMATE TLM ANALYSIS WITH IMPROVED ANALYSIS  
FOR SAMPLE P-DIFFUSED ( $L = 47.2 \mu\text{m}$ )

Parameter	Approximate TLM Analysis	Improved TLM Analysis
$R_{sh} (\Omega/\square)$	142	$143 \pm 1.1\%$
$L_T (\mu\text{m})$	61.2	$60.7 \pm 15\%$
$\rho_c (\text{m}\Omega\text{-cm}^2)$	5.34	$5.26 \pm 32\%$
$L_T/L$	1.30	1.29

approximate analysis.) The approximate contact resistivity ( $4.37 \text{ m}\Omega\text{-cm}^2$ ) is 25% higher than the improved value ( $3.51 \text{ m}\Omega\text{-cm}^2$ ) for the p-TOPCon sample. It is always the case that the approximate value is higher than the improved value because the improved analysis allows for some transfer of current to the zero-resistance metal bar.

A similar tabulation for the other two contact systems is given in Tables V and VI. For the n-TOPCon sample of Table V, the approximate contact resistivity ( $1.98 \text{ m}\Omega\text{-cm}^2$ ) is considerably higher than the improved value ( $0.89 \text{ m}\Omega\text{-cm}^2$ ), which also includes an attempt to account for 2-D current flow, as described below. For the p-diffused sample of Table VI, the approximate contact resistivity ( $5.34 \text{ m}\Omega\text{-cm}^2$ ) is 1.5% higher than the improved value ( $5.26 \text{ m}\Omega\text{-cm}^2$ ). Note also that the current transfer length obtained by measurement and analysis can be greater than the physical contact length ( $L_T/L > 1$ ).

Analysis of the n-TOPCon sample, as summarized in Table V, merits further remarks. As noted in Table I, the structure is:  $\text{Ag}/\text{SiN}_x/\text{n}^+$  poly/tunnel oxide/ $n$ -substrate. Unlike the p-TOPCon and the p-diffused samples, there is no p-n junction isolation to confine the measuring current to a thin (submicron) layer near the surface to justify a 1-D analysis. For n-TOPCon, the current flows through the entire thickness ( $180 \mu\text{m}$ ) of the sample, which is approximately three times  $L_T$  ( $61.3 \mu\text{m}$ ). This

TABLE VII  
CONTRIBUTION OF CONTACT RESISTIVITY TO CELL SERIES RESISTANCE AND  
CORRESPONDING LOSS OF FILL FACTOR AND EFFICIENCY

Sample	$\rho_c (\text{m}\Omega\text{-cm}^2)$	$r_{series} (\Omega\text{-cm}^2)$	$\Delta\text{FF}$	$\Delta\eta (\%)$
p-TOPCon	3.51	0.082	-0.00407	-0.102
n-TOPCon	0.89	0.015	-0.00072	-0.018
p-diffused	5.26	0.178	-0.00883	-0.221

calls for a 2-D analysis in order to obtain accurate results. Such an analysis has been reported for contacts applied directly to a thick sample [17]. Guided by this 2-D approach, an effort was made to improve the accuracy of the n-TOPCon results. The approach was to add the effect of the  $n^+$  poly layer in parallel with the n-substrate to the previous 2-D analysis [17] while matching the results of the 1-D analysis ( $\rho_c$  of  $1.65 \text{ m}\Omega\text{-cm}^2$  and  $R_{sh}$  of  $43.9 \Omega/\square$ ). This required an n-substrate resistivity of  $1.03 \Omega\text{-cm}$  ( $57 \Omega/\square$ ), which is within the 1–3  $\Omega\text{-cm}$  range of starting wafer resistivity, and an  $n^+$  poly layer with sheet resistance of  $190 \Omega/\square$ , which is not unreasonable, to give a parallel sheet resistance of  $43.9 \Omega/\square$ . The  $\text{Ag}/\text{n}^+$  poly contact resistivity was estimated in this way to be  $0.89 \text{ m}\Omega\text{-cm}^2$ , with the additional resistance associated with the longer 2-D current path inflating the apparent contact resistivity to the  $1.65 \text{ m}\Omega\text{-cm}^2$  value obtained with the faulty 1-D analysis.

The tunnel oxide may also introduce an additional resistance which would artificially inflate the  $\rho_c$  value obtained in a 1-D analysis, but the magnitude of this effect is not known and was not considered. Admittedly, the analysis method used to arrive at the  $0.89\text{-m}\Omega\text{-cm}^2$  value in Table V is fraught with uncertainty because of unknown wafer resistivity, unknown effect of the tunneling oxide, and unverified validity of the parameter-matching approach. The improved  $\rho_c$  value in Table V ( $0.89 \text{ m}\Omega\text{-cm}^2$ ) is presented only as a rough estimate of the true value. More sophisticated analysis, aided by 2-D simulations and a proper assessment of the role of the tunneling oxide, is needed for a reliable analysis of the n-TOPCon structure. Such an analysis could be the subject of future research, but is considered beyond the scope of this work. The improved analyses for the p-TOPCon and p-diffused samples of Tables IV and VI, however, are considered reliable because in these cases, the measuring current is confined to the  $p^+$  layer by p-n junction isolation and does not flow into the n-substrate or across the tunneling oxide.

The contribution of contact resistivity to the cell series resistance ( $r_{series}$ ), as calculated from (11), is given in Table VII for the most reliable  $\rho_c$  values. This component of series resistance causes a loss in fill factor relative to the ideal case of zero contact resistivity given by [18, pp. 220–222]

$$\Delta\text{FF} = -(J_{sc}/V_{oc}) r_{series}(\text{contact}) \text{FF}_{ideal} \quad (20)$$

where  $J_{sc}$  and  $V_{oc}$  are cell short-circuit current density and open-circuit voltage, and  $\text{FF}_{ideal}$  is the resistance-free fill factor (pseudo fill factor in a  $\text{Suns-}V_{oc}$  measurement). Typical values give  $\Delta\text{FF} \approx -(0.0496/\Omega\text{-cm}^2) r_{series}(\text{contact})$ . The associated loss in efficiency ( $\Delta\eta$ ) relative to the ideal case of zero contact resistivity is also estimated and entered in Table VII. Note that

TABLE VIII

APPROXIMATE TLM CONTACT RESISTIVITY AND ERROR RELATIVE TO TRUE VALUE CALCULATED FOR  $L_T/L$  RATIOS RANGING FROM 0.1 TO 4.0 WITH UNCONTACTED BARS ISOLATED FROM SHEET (CONVENTIONAL CASE) ( $L = 50 \mu\text{m}$ ,  $R_{sh} = 100 \Omega/\square$ ,  $R_{bar} = R_{sh}(L/Z)$ )

$L_T$ ( $\mu\text{m}$ )	$L_T/L$	$\rho_{c\text{-true}}$ ( $\text{m}\Omega\text{-cm}^2$ )	$\rho_{c\text{-approx}}$ ( $\text{m}\Omega\text{-cm}^2$ )	$(\rho_{c\text{-approx}} - \rho_{c\text{-true}})/\rho_{c\text{-true}}$ (%)
5.0	0.10	0.025	0.570	2200%
12.5	0.25	0.156	0.595	280%
15.6	0.31	0.244	0.631	160%
18.8	0.38	0.352	0.690	96%
25.0	0.50	0.625	0.881	41%
37.5	0.75	1.406	1.554	10%
50.0	1.00	2.500	2.592	3.7%
75.0	1.50	5.625	5.668	0.77%
100	2.00	10.00	10.02	0.25%
150	3.00	22.50	22.51	0.05%
200	4.00	40.00	40.01	0.02%

$\Delta\eta$  is as large as  $-0.221\%$  (absolute) for the samples studied. If the contact resistivity could be reduced, some of this loss would be reclaimed and the measured cell efficiency would increase accordingly up to a limiting value of  $0.221\%$ .

Gridline resistance was measured by the busbar-to-busbar method in order to compare it with the contact resistance. A 5 mm length of gridline has a resistance of  $26.4 \mu\Omega$  for the n-TOPCon sample and  $30.2 \mu\Omega$  for the p-diffused sample. Contact resistance for a 5 mm length of gridline is  $0.538 \Omega$  ( $R_c = \rho_c/ZL_T$ ) for the n-TOPCon sample and  $2.23 \Omega$  ( $R_c = \rho_c/ZL$ ) for the p-diffused sample. The ratio of gridline resistance to contact resistance is then  $4.90 \times 10^{-5}$  and  $1.35 \times 10^{-5}$ . These are appropriate values, since the current probe is placed in the middle of a 10 mm (nominal) long gridline in a TLM measurement. Such low ratios mean that the measuring current flows easily from the current probe along the TLM gridline and then passes uniformly across the contact interface. This ensures a 1-D current flow through the gridline TLM pattern and avoids issues related to sample width and line resistance, as cautioned in [19] and [20].

#### IV. ERROR ANALYSIS OF APPROXIMATE APPROACHES

Data from the previous section showed that approximate TLM analysis gives a  $\rho_c$  value that is  $1.5\%$  to  $25\%$  higher for the samples measured than that given by the exact TLM analysis, with the difference (error) becoming larger as  $L_T/L$  becomes smaller. In order to quantify the error incurred by using the approximate analysis, calculations were carried out for a representative gridline TLM contact system: gridline pitch ( $p$ ) 1.50 mm, contact length ( $L$ )  $50 \mu\text{m}$ , spacing ( $s$ ) 1.45 mm, sample width ( $Z$ ) 10 mm, and silicon sheet resistance ( $R_{sh}$ )  $100 \Omega/\square$ . For each value of current transfer length ( $L_T$ ), five  $R_n$  values were calculated from (8) so as to include the effect of uncontacted bars, with  $n = 1$  to 5. These five “data points” were fit to a straight line to determine  $R_{sh}$  and  $L_T$  using either (17) with ( $d_n$ ,  $R_n$ ) points for an approximate analysis or (8) with ( $n$ ,  $R_n$ ) points for an exact analysis.

Results of these calculations for  $L_T/L$  ranging from 0.1 to 4.0 are given in Table VIII, which also shows the true value

Relative Error in Calculated  $\rho_c$  vs.  $L_T/L$   
(Approximate treatment of uncontacted gridlines)

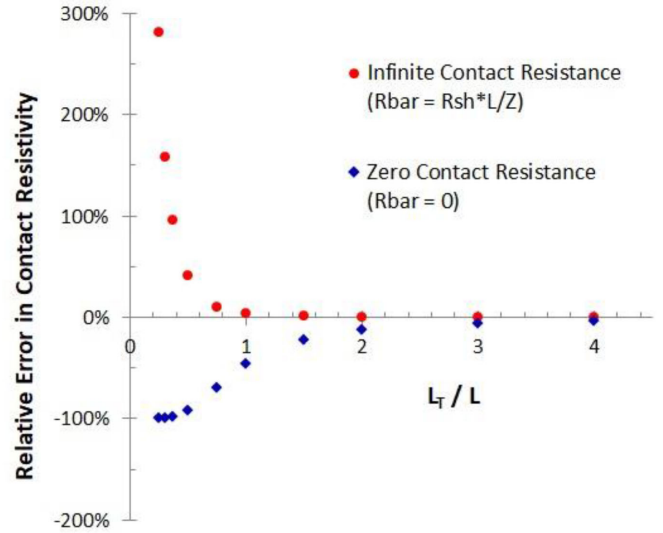


Fig. 7. Error in contact resistivity as determined by two approximate analyses as a function of  $L_T/L$ . In both cases, the error rapidly becomes large for  $L_T/L < 1$ .

of  $\rho_c$  from (1). In all cases,  $\rho_c$  from the exact analysis of the “data” agreed very well with the true value, as expected. The value of  $\rho_c$  obtained by an approximate TLM analysis agreed well with the true value for  $L_T/L \geq 1$  as shown by the error parameter in the right column of Table VIII. However, for  $L_T/L < 1$ , the error is significant, e.g.,  $10\%$  at  $L_T/L = 0.75$ ,  $41\%$  at  $L_T/L = 0.50$ , and  $280\%$  at  $L_T/L = 0.25$ . As the contact becomes better, the approximate gridline TLM analysis delivers a  $\rho_c$  value with progressively greater error, whereas the exact gridline TLM analysis reproduces the true  $\rho_c$  values in all cases. The exact  $\rho_c$  is always less than the approximate  $\rho_c$ . The approximate analysis in this case assumes no current transfer between the sheet and the uncontacted gridlines. This is equivalent to assuming an infinite contact resistance between the sheet and the floating gridlines. These results are shown graphically by the dots in Fig. 7.

The approximate analysis described above is that which is normally applied to gridline TLM data [6]. A second approximate analysis could be considered where the uncontacted gridlines are in intimate contact (zero contact resistance) with the sheet. With zero contact resistance and zero gridline resistance, the resistance associated with a floating gridline is zero [7]. Results of this second approximate analysis are given in Table IX and indicated by the diamond symbols in Fig. 7. In this case, the approximate analysis underestimates the true  $\rho_c$ , particularly for  $L_T/L < 1$ .

The question of uncertainty in the value of  $\rho_c$  derived from noisy gridline TLM data arises. The 30 ( $n$ ,  $R_n$ ) data points for sample p-TOPCon (see Table II) were examined by calculating the standard deviation of all resistance values for a given  $n$ . A weighted average of these standard deviations was computed, weighted by the number of resistance values for each  $n$  (e.g., 8 values for  $n = 2$ ). The same calculation was done for the 30 points

TABLE IX

APPROXIMATE TLM CONTACT RESISTIVITY AND ERROR RELATIVE TO TRUE VALUE CALCULATED FOR  $L_T/L$  RATIOS RANGING FROM 0.1 TO 4.0 WITH ZERO CONTACT RESISTANCE FOR UNCONTACTED BARS ( $L = 50 \mu\text{m}$ ,  $R_{sh} = 100 \Omega/\square$ ,  $R_{bar} = 0$ )

$L_T$ ( $\mu\text{m}$ )	$L_T/L$	$\rho_{c\text{-true}}$ ( $\text{m}\Omega\text{-cm}^2$ )	$\rho_{c\text{-approx}}$ ( $\text{m}\Omega\text{-cm}^2$ )	$(\rho_{c\text{-approx}} - \rho_{c\text{-true}})/\rho_{c\text{-true}}$ (%)
5.0	0.10	0.025	$2.01 \times 10^{-10}$	-100%
12.5	0.25	0.156	$2.08 \times 10^{-4}$	-100%
15.6	0.31	0.244	$1.59 \times 10^{-3}$	-99%
18.8	0.38	0.352	$6.71 \times 10^{-3}$	-98%
25.0	0.50	0.625	$4.63 \times 10^{-2}$	-93%
37.5	0.75	1.41	0.426	-70%
50.0	1.00	2.50	1.36	-46%
75.0	1.50	5.62	4.40	-22%
100	2.00	10.0	8.75	-12%
150	3.00	22.5	21.2	-5.6%
200	4.00	40.0	38.7	-3.2%

Simulated Resistance Data with Noise

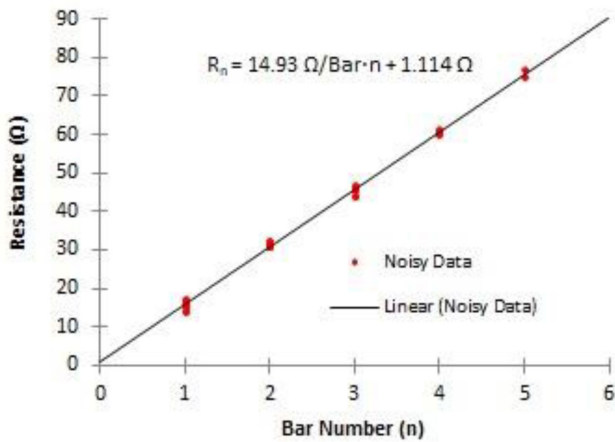


Fig. 8. Plot of 30 ( $n, R_n$ ) simulated data points with added noise (mean  $0 \Omega$ , standard deviation  $0.97 \Omega$ ) for exact gridline TLM analysis showing resultant scatter of data points.

for sample n-TOPCon and the 30 points for sample p-diffused. It appears that the variation in resistance values (noise) is related more to contact resistance than to sheet resistance, since the standard deviation was roughly the same for all five groups ( $n = 1$  to  $5$ ) for a given sample. Since the three weighted standard deviations averaged to  $0.97 \Omega$ , noise in the resistance values was represented by a normal distribution with average of  $0 \Omega$  and standard deviation of  $0.97 \Omega$ . A simulated set of 30 data points (10 for  $n = 1$ , 8 for  $n = 2$ , 6 for  $n = 3$ , 4 for  $n = 4$ , and 2 for  $n = 5$ ) was then created for a given  $L_T/L$  value with all other simulation parameters as given above. To each of the 30 resistance values, noise was added at random from the normal distribution. An example is shown in Fig. 8, with  $L = 50 \mu\text{m}$ ,  $L_T/L = 1$ , and  $R_{sh} = 100 \Omega/\square$ .

Results of the calculations with noise are summarized in Table X. Each calculation represents a “measurement” of a gridline TLM sample with exact analysis. The average “measured” contact resistivity along with its standard deviation on a single “measurement” is given for each of the three  $L_T/L$

TABLE X

SUMMARY OF CALCULATIONS WITH NOISE

$L_T/L$	$\rho_{c\text{-true}}$ ( $\text{m}\Omega\text{-cm}^2$ )	# Calculations	$\langle \rho_{c\text{-noise}} \rangle$ ( $\text{m}\Omega\text{-cm}^2$ )
0.5	0.625	10	$0.36 \pm 1.04$
1.0	2.5	5	$2.54 \pm 0.52$
2.0	10	5	$10.01 \pm 0.95$

values examined. Since all three standard deviations average to  $\pm 0.84 \text{ m}\Omega\text{-cm}^2$ , it appears that the “measurement” is valid down to about  $1 \text{ m}\Omega\text{-cm}^2$  with the level of noise assumed. However, it should be kept in mind that noise is random, and its effect is reduced as more measurements are made with multiple gridline TLM samples cut from the same cell. Thus, with exact TLM analysis, such an average contact resistivity can be quite accurate if a large enough number of measurements are made. With an approximate TLM analysis, however, a systematic error (see Fig. 7) remains regardless of the number of measurements made. Of course, if the contact can be made more uniform (e.g., laser-defined plated Ni/Cu contacts), then the limit imposed by noise on minimum contact resistivity that can be measured accurately is reduced.

## V. DISCUSSION

It is possible to infer contact resistivity associated with the contact grid of a finished solar cell without making a TLM measurement, provided the remaining components of cell series resistance can be determined independently and provided  $L_T \geq L/2$  [21]. However, a conventional TLM test pattern with bars having variable spacing remains the standard technique for determining contact resistivity, and is frequently employed in the research stage of contact development [22], [23]. Many possibilities exist for novel contact systems, where the product  $J_{0c} \rho_c$  is an important figure of merit [24]. As a given contact technology matures and is implemented in solar cells, it is often more convenient and representative to use a gridline TLM pattern than a conventional TLM pattern. Developments in this article show that by including the effects of uncontacted bars (gridlines), a more accurate determination of contact resistivity can be made with the gridline TLM pattern.

In [25], for example, it is stated that part of the reason the efficiency of a prototype passivated emitter and rear cell (PERC) production cell (156 mm) increased to 22.61% was that the contact resistivity of the screen-printed front Ag contact had improved to  $4.40 \text{ m}\Omega\text{-cm}^2$ . This value was apparently determined from measurements of special gridline TLM patterns where the width of the gridlines ( $L$ ) was  $200 \mu\text{m}$ —considerably greater than for a normal cell to facilitate probing. A selective emitter was employed with the field portion ( $n^+$ ) etched back to  $130 \Omega/\square$ , so the contact portion ( $n^{++}$ ) is assumed to be  $\approx 80 \Omega/\square$ . By (1), this combination of  $\rho_c$  and  $R_{sh}$  in the contact region gives  $L_T$  of  $74 \mu\text{m}$ , so  $L_T/L = 0.37$ . According to Table VIII, such a low  $L_T/L$  ratio requires a significant correction to  $\rho_c$  assuming an approximate gridline TLM analysis was used to arrive at the  $\rho_c$  value stated. After correcting for uncontacted bars (gridlines),  $\rho_c$  decreases from  $4.40 \text{ m}\Omega\text{-cm}^2$  (assumed approximate analysis)

to  $2.24 \text{ m}\Omega\cdot\text{cm}^2$  (exact analysis)—a significant reduction. This more accurate value is needed for careful cell evaluation.

Although screen-printed Ag contacts are ubiquitous in production solar cells, other contact materials and processes are being investigated as alternatives. One such contact system is Ni/Cu plated into laser contact openings. This contact system allows for quite narrow lines ( $L < 30 \text{ }\mu\text{m}$ ) with  $\rho_c < 1 \text{ m}\Omega\cdot\text{cm}^2$ . For example, a Ni/Cu contact plated onto a  $90 \text{ }\Omega/\square$   $n^+$  emitter gave  $\rho_c$  of  $0.4 \text{ m}\Omega\cdot\text{cm}^2$  [7]. From (1), this indicates  $L_T$  of  $21 \text{ }\mu\text{m}$ . Similarly, a Ni/Cu contact plated onto a  $140 \text{ }\Omega/\square$   $p^+$  emitter gave  $\rho_c$  of  $0.53 \text{ m}\Omega\cdot\text{cm}^2$  [26], which corresponds to  $L_T$  of  $20 \text{ }\mu\text{m}$  in a 22.9% large-area cell. A gridline TLM pattern was used in both cases. With these low  $L_T$  values,  $L_T/L$  could well be  $< 1$ , which then requires an improved gridline TLM analysis to arrive at an accurate  $\rho_c$  value for such plated Ni/Cu contacts.

Other contact systems have even lower values of  $\rho_c$  and  $L_T$ . For example, an evaporated Ti/Pd/Ag contact (sometimes used for research cells) had  $\rho_c$  of  $0.005 \text{ m}\Omega\cdot\text{cm}^2$  when applied to a  $60 \text{ }\Omega/\square$   $n^+$  emitter [8, p. 650]. This gives an  $L_T$  value of just  $2.9 \text{ }\mu\text{m}$ . Silicide contacts can have yet lower values of  $\rho_c$  and  $L_T$ .  $\text{TiSi}_2$  contacting a  $200 \text{ }\Omega/\square$   $p^+$  diffusion layer had  $\rho_c$  of  $0.001 \text{ m}\Omega\cdot\text{cm}^2$  [10, p. 566] to give an  $L_T$  value of  $0.71 \text{ }\mu\text{m}$ . NiSi and PtSi had  $\rho_c$  values ranging from 0.1 to  $0.00001 \text{ m}\Omega\cdot\text{cm}^2$  depending on the dopant concentration at the contacted silicon surface [11]. Alloyed Al contacts to Si  $p^+$  (Al) are also expected to have very low  $\rho_c$ . The point is that any contact with  $L_T/L < 1$  and measured using a gridline TLM pattern should, for accuracy, have an exact analysis of the data to explicitly include the effect of uncontacted gridlines.

## VI. SUMMARY

Contact resistance needs to be considered in the design and analysis of solar cells because, like any resistance, it robs power from the cell and must be minimized. A gridline TLM pattern, cut as a strip from the finished cell, is often used to measure contact resistivity and sheet resistance. This pattern, although convenient to use, can yield inaccurate results for  $\rho_c$  because data analysis (as currently practiced) ignores uncontacted (floating) gridlines. In reality, some current does transfer into and out of the uncontacted gridlines, so the usual analysis of gridline TLM data delivers only approximate values of  $\rho_c$  and  $R_{sh}$ . In this article, a refinement has been developed that takes the uncontacted gridlines explicitly into account, thereby delivering more accurate values of  $\rho_c$  and  $R_{sh}$  at the expense of a somewhat more complex numerical analysis of the TLM data. This improved accuracy is accomplished by including the resistance associated with an uncontacted bar (gridline) in the pattern as:  $R_{\text{bar}} = (2L_T/Z) R_{sh} \tanh[L/(2L_T)]$ . Ignoring uncontacted gridlines in the approximate analysis does not introduce significant error in  $\rho_c$  if  $L_T/L > 1$  but does if  $L_T/L < 1$ , with the error becoming progressively larger as  $L_T/L$  becomes smaller. The improved analysis described in this article always gives lower contact resistivity and slightly higher sheet resistance than the conventional approximate analysis with  $R_{\text{bar}} = (L/Z) R_{sh}$ .

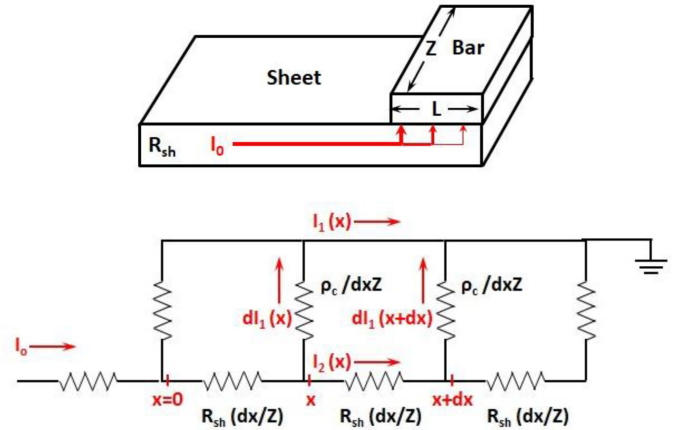
Measurements were made on gridline TLM samples for three different contact systems currently under development. These systems include an n-type TOPCon structure, a p-type TOPCon

structure, and a contact to a p-type emitter, each using a commercially available Ag paste. In every case, the gridline TLM data underwent both an approximate analysis and an improved analysis to determine  $\rho_c$ . The two analyses were compared, and the approximate analysis showed an error ranging from 1.5% to 25% in  $\rho_c$ . (In the n-TOPCon case, current flow is not strictly 1-D since some current flows in the relatively thick substrate as well as the thin  $n^+$  layer, thereby introducing a significant error in the analysis. This was addressed by applying a methodology from a published 2-D analysis.) In addition, calculations were carried out to quantify the error in  $\rho_c$  introduced by two approximate analyses as a function of  $L_T/L$ . Further calculations examined the impact of noise in the measured resistance values on the uncertainty of measured  $\rho_c$ .

A well-designed contact has  $L_T/L < 1$ , and so stands to benefit from an improved analysis of gridline TLM data. Other contacts to Si (e.g., plated Ni/Cu, Ti/Pd/Ag,  $\text{TiSi}_2$ , alloyed Al) typically have lower contact resistivity than screen-printed and fired Ag, and so may benefit from this type of analysis as well.

## APPENDIX

Derivation of  $R_c = R_{sh} \frac{L_T}{Z} \coth \frac{L}{L_T}$  using TLM.



$I_1(x)$  = current in contact bar at location  $x$ .

$I_2(x)$  = current in silicon sheet at location  $x$ .

Kirchoff's Law:  $\sum V_i = 0$  around a closed loop.

Summing voltages, beginning at  $x$  and going clockwise around a closed loop gives

$$-dI_1(x) \frac{\rho_c}{dxZ} + dI_1(x+dx) \frac{\rho_c}{dxZ} + I_2(x) R_{sh} \frac{dx}{Z} = 0$$

$$\rho_c \frac{d^2 I_1(x)}{dx^2} + I_2(x) R_{sh} = 0$$

$$I_1(x) + I_2(x) = I_0$$

$$\frac{d^2 I_1(x)}{dx^2} - \frac{R_{sh}}{\rho_c} I_1(x) = -\frac{R_{sh}}{\rho_c} I_0.$$

$$\text{Define } L_T^2 = \frac{\rho_c}{R_{sh}}$$

$$\frac{d^2 I_1(x)}{dx^2} - \frac{1}{L_T^2} I_1(x) = -\frac{I_0}{L_T^2}.$$

Two boundary conditions (current in bar) are given as

$$\begin{aligned}
 I_1(x=0) &= 0 \\
 I_1(x=L) &= I_0 \\
 I_1(x) &= I_0 \left[ \frac{e^{(x-L)/L_T} - e^{-(x-L)/L_T}}{e^{L/L_T} - e^{-L/L_T}} + 1 \right] \\
 V_0 &= \frac{\rho_c}{dxZ} dI_1(x=0) = \frac{\rho_c}{Z} \frac{dI_1(x)}{dx} \Big|_{x=0} \\
 V_0 &= \frac{\rho_c}{Z} \frac{1}{L_T} I_0 \coth \frac{L}{L_T} \\
 R_c &= \frac{V_0}{I_0} = \frac{\rho_c}{Z} \frac{1}{L_T} \coth \frac{L}{L_T} \\
 R_c &= R_{sh} \frac{L_T}{Z} \coth \frac{L}{L_T} \text{ (QED)}.
 \end{aligned}$$

#### ACKNOWLEDGMENT

The authors gratefully acknowledge the Heraeus R&D staff for preparing and measuring the gridline TLM samples used in this study and the reviewers for their insightful comments and recommendations.

#### REFERENCES

- [1] W. Shockley, "Research and investigation of inverse epitaxial UHF power transistors," Air Force Avionics Lab., Wright-Patterson Air Force Base, OH, USA, Tech. Documentary Rep. AL TDR 64-207P, 1964.
- [2] H. H. Berger, "Contact resistance on diffused resistors," in *Proc. IEEE Int. Solid-State Circuits Conf., Dig. Tech. Papers*, Feb. 1969, vol. 12, pp. 160–161.
- [3] D. K. Schroder and D. L. Meier, "Solar cell contact resistance—A review," *IEEE Trans. Electron Devices*, vol. ED-31, no. 5, pp. 637–647, May 1984.
- [4] D. K. Schroder, *Semiconductor Material and Device Characterization*, 3rd ed. Hoboken, NJ, USA: Wiley-Interscience, 2015, pp. 147.
- [5] A. M. Gabor *et al.*, "Dependence of solar cell contact resistivity measurements on sample preparation methods," in *Proc. 43rd Photovolt. Spec. Conf.*, Jun. 2016, pp. 3033–3036.
- [6] R. Janoch, A. M. Gabor, A. Anselmo, and C. E. Dube, "Contact resistance measurement—Observations on technique and test parameters," in *Proc. 42nd Photovolt. Spec. Conf.*, Jun. 2015, doi: [10.1109/PVSC.2015.7355851](https://doi.org/10.1109/PVSC.2015.7355851).
- [7] H. Mir, V. Arya, H. Höffler, and A. Brand, "A novel TLM analysis for solar cells," *IEEE J. Photovolt.*, vol. 9, no. 5, pp. 1336–1342, Sep. 2019.
- [8] D. L. Meier and D. K. Schroder, "Contact resistance: Its measurement and relative importance to power loss in a solar cell," *IEEE Trans. Electron Devices*, vol. ED-31, no. 5, pp. 647–653, May 1984.
- [9] D. B. Scott, W. R. Hunter, and H. Shichijo, "A transmission line model for silicided diffusions: Impact on the performance of VLSI circuits," *IEEE Trans. Electron Devices*, vol. ED-29, no. 4, pp. 651–661, Apr. 1982.
- [10] D. B. Scott *et al.*, "Titanium disilicide contact resistivity and its impact on 1- $\mu$ m CMOS circuit performance," *IEEE Trans. Electron Devices*, vol. ED-34, no. 3, pp. 562–574, Mar. 1987.
- [11] N. Stavitski *et al.*, "Evaluation of transmission line model structures for silicide-to-silicon specific contact resistance extraction," *IEEE Trans. Electron Devices*, vol. 55, no. 5, pp. 1170–1176, May 2008.
- [12] F. Feldmann, M. Bivour, C. Reichel, M. Hermle, and S. W. Glunz, "Passivated rear contacts for high-efficiency n-type Si solar cells providing high interface passivation quality and excellent transport characteristics," *Sol. Energy Mater. Sol. Cells*, vol. 120, pp. 270–274, 2014.
- [13] S. W. Glunz *et al.*, "Passivating and carrier-selective contacts—Basic requirements and implementation," in *Proc. 44th Photovolt. Spec. Conf.*, Jun. 2017, pp. 2064–2069.
- [14] "4-TEST tool originally from GP Solar and now from ISRA Vision," 2020. [Online]. Available: [www.isravision.com](http://www.isravision.com)
- [15] "ContactSpot tool from BrightSpot Automation," 2020. [Online]. Available: [www.brightspotautomation.com](http://www.brightspotautomation.com)
- [16] "TLM-SCAN tool from PV-Tools GmbH," 2020. [Online]. Available: [www.pv-tools.de](http://www.pv-tools.de)
- [17] S. Eidelloth and R. Brendel, "Analytical theory for extracting specific contact resistances of thick samples from the transmission line method," *IEEE Electron Device Lett.*, vol. 35, no. 1, pp. 9–11, Jan. 2014.
- [18] A. L. Fahrenbruch and R. H. Bube, *Fundamentals of Solar Cells*. New York, NY, USA: Academic, 1983.
- [19] G. Gregory *et al.*, "TCAD modeling of TLM contact resistance structures," in *Proc. 32nd Eur. Photovolt. Sol. Energy Conf.*, Jun. 2016, pp. 874–878.
- [20] S. Guo, G. Gregory, A. M. Gabor, W. V. Schoenfeld, and K. O. Davis, "Detailed investigation of TLM contact resistance measurements on crystalline silicon solar cells," *Sol. Energy*, vol. 151, pp. 163–172, Jul. 2017.
- [21] D. L. Meier, V. Chandrasekaran, A. Gupta, V. Yelundur, and A. Rohatgi, "Silver contact grid: Inferred contact resistivity and cost minimization in 19% silicon solar cells," *IEEE J. Photovolt.*, vol. 3, no. 1, pp. 199–205, Jan. 2013.
- [22] M. Leilaoui *et al.*, "Contact resistivity of the p-type amorphous silicon hole contact in silicon heterojunction solar cells," *IEEE J. Photovolt.*, vol. 10, no. 1, pp. 54–62, Jul. 2019.
- [23] W. Wang *et al.*, "An expanded Cox and Strack method for precise extraction of specific contact resistance of transition metal oxide/n-silicon heterojunction," *IEEE J. Photovolt.*, vol. 9, no. 4, pp. 1113–1120, Jan. 2020.
- [24] J. Melskens *et al.*, "Passivating contacts for crystalline silicon solar cells: From concepts and materials to prospects," *IEEE J. Photovolt.*, vol. 8, no. 2, pp. 373–388, Mar. 2018.
- [25] W. Deng *et al.*, "22.61% efficient fully screen printed PERC solar cell," in *Proc. 44th Photovolt. Spec. Conf.*, Jun. 2017, pp. 2220–2226.
- [26] F. Feldmann *et al.*, "Evaluation of TOPCon technology on large area solar cells," in *Proc. 33rd Eur. Photovolt. Sol. Energy Conf.*, 2017, pp. 465–467.